forum acusticum 2026
8-12 September · Graz, Austria

SIMULATION-BASED PREDICTION OF RIR MEASUREMENT LOCATIONS

Otavio Colella Gomes[1], Nils Peters[2]

[1] *Hochschule für Musik Detmold, Detmold, Germany*
[2] *Trinity College, The University of Dublin, Ireland*

This contribution has been accepted based on the submitted abstract. The submitted manuscript was not reviewed and is reproduced here without edits or corrections by the conference board. Neither the EAA nor the AAA take responsibility for its contents.

Abstract

The advent of robotic-aided acoustic measurements has enabled the precise acquisition of Room Impulse Responses (RIRs) across dense sampling grids, which is essential, e.g., for documenting the unique acoustics of cultural heritage sites and music venues. Despite these technological advances, capturing a high volume of RIRs in expansive spaces remains a time-intensive process, and determining the most salient measurement points would be ideal to optimize this process. This study investigates the use of basic room simulations to predict the necessary spatial density of RIR measurements. Our approach is perceptually driven, incorporating the Just Noticeable Differences (JNDs) of objective acoustic parameters, such as Early Decay Time (EDT) or Clarity (C_{80}). Our predictions are grounded in physical measurements from a high-density RIR dataset and benchmarked against a basic geometric-acoustic simulation of the same environment. Results of a case study show that such simulations can effectively approximate the required measurement locations. Moreover, the optimal resolution depends on the chosen objective metrics and their associated JNDs. Simulation-based prediction thus provides a practical framework for optimizing measurement strategies and reducing the time required for dense RIR acquisition.

Keywords: *Acoustic digital twin, Perception, Simulation*

1. Introduction

Robotic-aided room acoustic measurements are becoming more widespread [1–3] and facilitate RIR measurement campaigns in large spaces. However, measurement time and storage space are finite resources. Strategies for selecting measurement locations within a given space are still under development. For precise room acoustic measurements, ISO 3382 [4] includes recommendations on where to measure. It is recommended that the microphone(s) should be:

- at least 1.5 m away from the sound source.
- positioned at least half a wavelength away from any major reflecting surfaces, i.e., 1 m.
- spaced at least half a wavelength apart for the lowest frequency of interest, i.e., 2 m, to achieve reasonably independent measurements.
- placed at more than three positions and result in at least 12 independent source-microphone combinations.
- not placed in highly symmetrical positions due to room modes.

Stolz et al. [5] investigated various acoustic and perceptual optimization methods to enhance the efficiency of spatial room impulse response (SRIR) measurements using a mobile robotic platform. They demonstrated that both exploratory algorithms and pre-planned grids based on human auditory perception of the direct sound component can theoretically reduce the number of required measurement positions. The Maximum Allowed Error Method (MAEM) determines a set of measurement locations based on similarity thresholds: a new measurement location is only required if there are sufficiently large differences to existing measurement locations. In [5] these thresholds are a) a minimum source distance of 1 m; b) a maximum allowed distance change of 25 %; and c) a maximum allowed angular change of 5°. Although these thresholds are perceptually motivated and based on Just Noticeable Differences (JNDs) of the Minimum Audible Angle (MAA) and source distance, they have been derived from geometric source-receiver relationships, therefore only considering the perception of the Direct Sound without the influence of early reflection and reverberation of the space.

2. Methodology

Since existing approaches are primarily based on geometric relationships between sources, receivers, and large surfaces, we aim to extend these approaches

Corresponding author: *otavio.colella@gmail.com.*
Copyright: *©2026 Colella Gomes et al. This is an open-access article distributed under the terms of the Creative Commons Attribution 3.0 Unported License, which permits unrestricted use, distribution, and reproduction in any medium, provided the original author and source are credited.*

by also considering the acoustic properties of the room. These acoustic properties are usually unknown prior to the measurement. Therefore, we propose using a simplified computational model of the measurement room to simulate the sound propagation and estimate acoustic properties at a large number of virtual measurement points. Based on these simulations, perceptual metrics are approximated, which then inform the selection process of the measurement locations. The following section introduces two different methods which are then evaluated in Section 3.

2.1. Method A - Perceived Source Direction

The perceived Direction-of-Arrival (DOA) of a sound is determined within approx. 1 ms after the first arriving wavefront (i.e., the Direct Sound). This auditory principle is also known as summing localization [6]. Approximately 1 ms after the Direct Sound, the Precedence Effect [7] starts dominating and suppresses the arriving early reflections from impacting the perceived sound direction, albeit sometimes not completely [8]. Based on the principle of summing localization, a reflection arriving within 1 ms after the Direct Sound would likely contribute to the perceived DOA.

The time between the arrival of direct sound and first reflection is also termed Initial Time Delay Gap (ITDG) [9] and is known to contribute to acoustical intimacy. If the ITDG is below 5 ms and the first reflection arrives from the ceiling or from the floor, then the perceived azimuth direction would likely be preserved and loudness may even be enhanced [8]. If the first reflection arrives from a side wall, then the perceived direction may be lateralized and will differ from the geometrical sound direction.

Using an auditory localization model, we can estimate the perceived direction of the sound event and use it instead of the geometrical direction within MAEM.

2.2. Method B - JND-informed Regions

In contrast to Method A, which focuses on localization related cues within the direct sound and first 5 ms, Method B considers room acoustic parameters describing broader temporal and spatial characteristics of the room response. We use the reported JNDs of each parameter to identify perceptually relevant spatial variations. Given the exploratory nature of the experiment, we adopt a threshold of 2 JNDs, corresponding to 2 dB for Clarity (C_{80}) and 0.10 for Lateral Fraction (J_{LF}).

Based on these thresholds, we divided the receiver grid into regions where the total range of variation of parameter values did not exceed 2 JNDs. We performed this division using an adapted seeded region-growing procedure [10], where the available receiver position closest to the source was selected as the seed of each new region.

Starting from a seed, we evaluated its eight neighbouring receiver positions, and accepted a candidate only when its inclusion kept the complete range of values within the adopted threshold:

$$x_{\max,R} - x_{\min,R} \leq \tau, \tag{1}$$

where $x_{\max,R}$ and $x_{\min,R}$ are the maximum and minimum values within region R, and τ is the parameter-specific threshold of the 2 JNDs. When multiple candidates satisfied this condition, we first added the point producing the smallest increase in the regional range. We updated the candidate list by including the neighbours of the newly accepted point, and evaluated the complete list. We continued expanding the region until no adjacent position could be added without exceeding τ. We then selected again from the remaining unassigned positions the closest seed to the source, and repeated the process until the complete grid had been divided.

Following the initial division, we merged the spatially adjacent regions when the range of their combined values also remained within τ. Each resulting region therefore represents a spatially connected collection of receiver positions whose internal parameter variation does not exceed the adopted perceptual threshold.

Table 1: Parameters specified in ISO 3382 [4] and their just noticeable differences (JNDs).

Percept	Parameter	Symbol	JND
Perceived Reverb	Reverberation Time	RT_{60} [s]	5%
	Early Decay Time	EDT [s]	5%
Perceived Clarity	Clarity	C_{80} [dB]	1 dB
	Definition	D_{50}	0.05
	Center Time	T_s [ms]	10 ms
ASW	Lateral Fraction	J_{LF}	0.05

3. Experiments

To evaluate the concepts outlined in Section 2 we utilize measured RIRs from QMUL's Octagon Room published in a dataset by Stewart and Sandler [11]. As can be seen in Fig. 1a, the room has the shape of an octagon. The reported volume is ≈9500 m^3. The dataset includes B-format SRIRs and Omnidirectional RIRs which were measured on a 13 m x 13 m grid with 1 m spacing, resulting in 169 measured positions (see Fig. 1c).

3.1. Room Acoustic Simulation

We designed a simplified 3D model based on the documentation of the dataset and publicly available images of the Octagon Room. We approximated the curves of the vaulted ceiling and the top lantern by using planar surfaces with shallow angles. The model contains 133 flat surfaces, a volume of 7300 m^3, a total surface area of 2552 m^2 and a floor area of 435 m^2.

The room volume reported in the dataset is consistent with an approximate geometric estimate of a solid constructed as a 23 m extrusion of a regular octagon. The lower volume of the simulated model arises from the more detailed representation and simplification of the vaulted ceiling and upper lantern. Figure 1b shows the designed 3D model from the inside.

We selected four materials for the simplified 3D model. Gray represents concrete, brown the wooden surfaces, light blue the windows and dark blue the bookshelves.

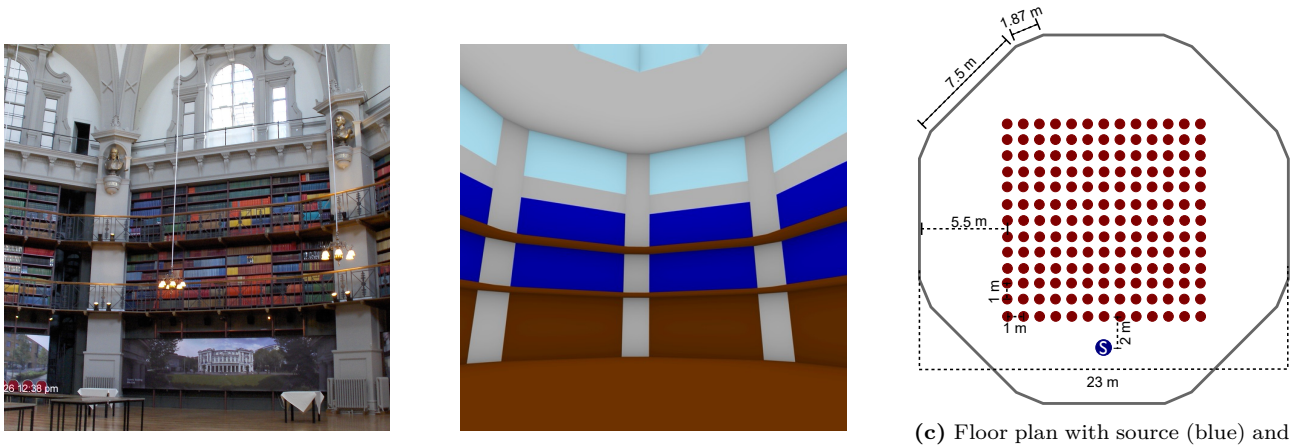

(a) The room as documented in [11]

(b) Interior view of the 3D model

(c) Floor plan with source (blue) and receiver positions (red).

Figure 1: The Octagon Room used for our experiments

We first assigned the materials properties to plausible values collected from [12] and [13]. We then calibrated the simulation for one receiver position by adjusting the absorption coefficients of the surfaces to match the simulated reverberation time to the measured data. Early Decay Time (EDT) was chosen for the calibration procedure as it is more sensitive to room geometry [14] and is accepted as a better predictor for reverberance [15]. Table 2 provides the absorption and scattering coefficients for the calibrated simulation. We set the scattering coefficients for each octave band according to the frequency-dependent scattering functions presented in [16]. The calibrated EDT and the measurement are displayed in Fig. 2.

Table 2: Material data used in the acoustic simulations.

Material	125 Hz	250 Hz	500 Hz	1 kHz	2 kHz	4 kHz
Absorption Coefficients						
Concrete	0.14	0.05	0.01	0.01	0.04	0.02
Wood	0.18	0.17	0.10	0.04	0.08	0.02
Glass	0.38	0.24	0.03	0.23	0.02	0.02
Bookshelves	0.86	0.90	0.95	0.75	0.70	0.75
Scattering Coefficients						
Concrete	0.01	0.01	0.02	0.04	0.08	0.10
Wood	0.01	0.03	0.07	0.15	0.27	0.32
Glass	0.01	0.02	0.02	0.06	0.12	0.15
Bookshelves	0.02	0.06	0.22	0.40	0.51	0.56

We conducted room acoustical simulations in RAVEN, a geometric acoustic (GA) software that combines ray tracing and image source method [17]. We positioned the source and receivers in the same locations as in the measurement dataset. The simulation settings were: 200000 particles, image source order up to 3, detection sphere of 1 m and filter length of 10 s.

To approximate the directivity of the acoustic source used in the measured data set, we converted the measured directivity of a Genelec 8331A reported in [18] to the OpenDAFF format and imported it into RAVEN. For each receiver position, we exported the resulting impulse responses as B-format SRIRs and omnidirectional RIRs. We also exported the room acoustic parameters calculated by RAVEN to be used in the subsequent analysis.

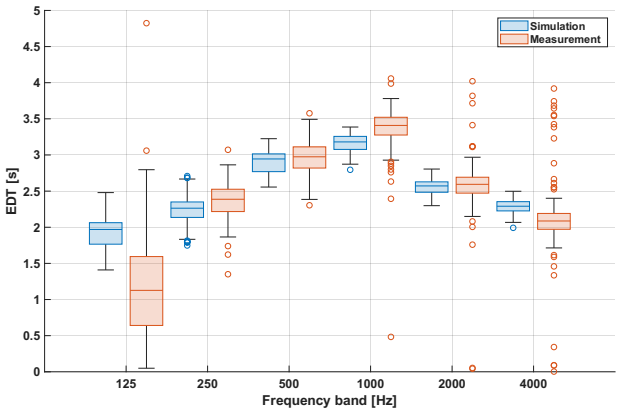

Figure 2: Measured (orange) and simulated (blue) EDT in six octave bands from 125 Hz to 4000 Hz after calibration.

3.2. Experiment A - Perceived Source Direction

To compare the perceived source direction with the geometric source direction, we utilize the binaural localization model by Dietz, Ewert, and Hohmann [19] implemented in the auditory modeling toolbox (AMT) [20]. The B-format SRIRs are converted into BRIRs using the KU-100 dummy head HRIRs from the SADIE II database [21]. Prior to BRIR conversion, we estimated the DOA of the Direct Sound from the B-format SRIRs using the SDM toolbox [22] and rotated the SRIRs to correct for DOA deviations (e.g., due to slight orientation offsets of the Soundfield microphone during measurements) using the known geometric source direction. The perceived source directions as estimated by the auditory model are illustrated in Fig. 3. The perceived directions start to deviate from the geometric source direction (grey arrows) for lateral directions, especially for front-lateral positions. Figure 3 further indicates small deviations between the simulated and measured BRIRs primarily for some front-lateral positions.

Using the perceived DOAs and the sound intensity (measured from the W-channel of the B-format SRIRs) we can evaluate the feasibility of using these data for the MAEM algorithm. We defined three MAEM conditions as summarized in Tab. 3 with the same

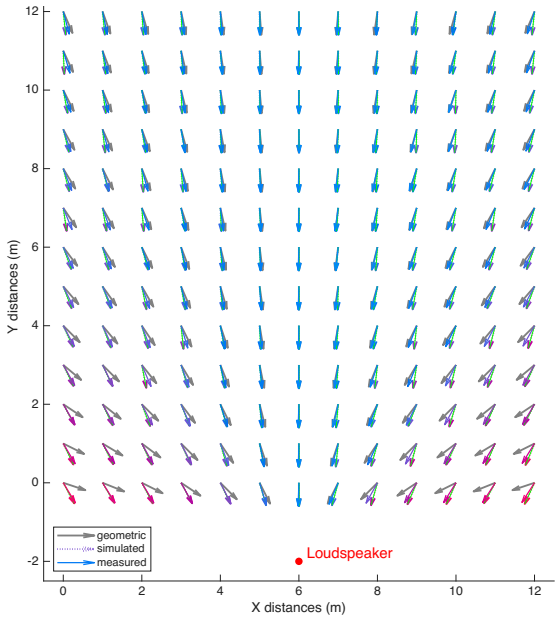

Figure 3: Difference between the geometric DOA and the perceived DOA as estimated with an auditory model from the simulated and measured BRIRs. Color of arrows illustrate the difference to the geometric source direction.

MAEM thresholds as defined in [5] and added a maximum allowed threshold for Sound Intensity changes of 1.5 dB. We compare the total number of the resulting directional regions for simulated and measured data and also compute the Pearson correlation coefficients ρ of the assigned region indices between simulated and measured locations as a proxy for similarity.

Table 3: MAEM conditions evaluated in Experiment A.

Objective and Threshold	Cond. 1	Cond. 2	Cond. 3
Geometric DOA, 5°	x		
Perceived DOA, 5°		x	x
Source Distance, 25 %	x	x	
Sound Intensity, 1.5 dB			x

Table 4 summarizes the results, for the cases when considering only the Direct Sound (RIR <1 ms) and the first 5 ms (RIR <5 ms). Condition 1, our baseline, as it depends only on geometrical source-receiver relations, led to 73 regions. Figure 4 shows the resulting region maps for the simulated and measured data for Condition 3 with RIRs up to 5 ms. Although the number of regions increases from simulation (44) to measured data (55), a good alignment between the simulated and measured data can be observed.

Table 4: Number of predicted regions and the correlation between simulated and measured results.

Cond.	RIR Portion	Number of Regions Simulated	Measured	ρ
1	-	73		-
2	<1ms	38	48	.97
	<5ms	40	49	.97
3	<1ms	48	58	.88
	<5ms	44	55	.92

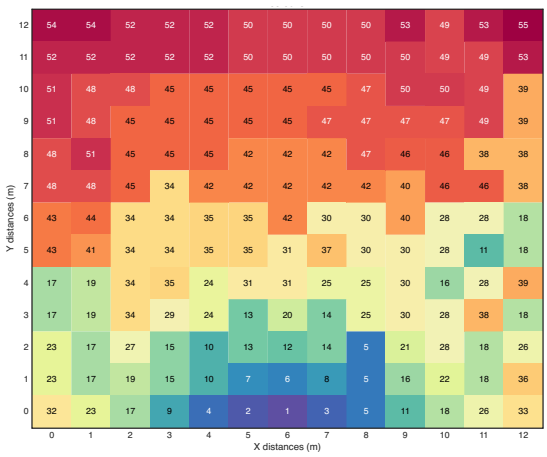

(a) Simulation

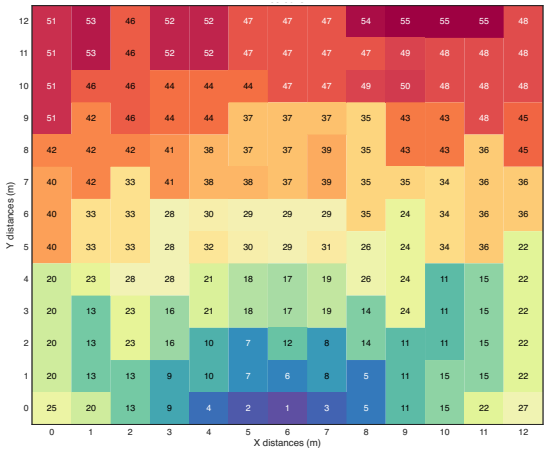

(b) Measurement

Figure 4: Regions for MAEM Condition 3 with RIR <5 ms.

3.3. Experiment B - JND-informed Regions

Figure 5 presents the measured and simulated ISO single number values of C_{80}, calculated as the average of the 500 Hz and 1000 Hz octave bands. The color of each cell represents the C_{80} value, while the number identifies the different JND-informed regions.
Both datasets have the highest C_{80} values in the central area close to the position of the acoustic source with lowest values on the sides of the receiver grid. The main spatial gradient is therefore present in both data, however, the measured dataset has more local variations that are not reproduced by the simulation. In comparison, the simulation has a smoother and regular distribution.
The measured data was divided into 11 regions, whereas the simulated data was divided into only 9 regions. The simulation, therefore, produced fewer and larger regions, however, the main subdivision around the high C_{80} area near the source is visible in both datasets.
Figure 6 shows measured and simulated ISO single number values of lateral fraction (J_{LF}), calculated as the average across the 125 Hz to 1000 Hz octave bands. Both figures show an increase in J_{LF} toward the far end of the receiver grid. However, the variation of the spatial distribution is stronger for J_{LF} than for C_{80}. Both figures present a similarly large region close to

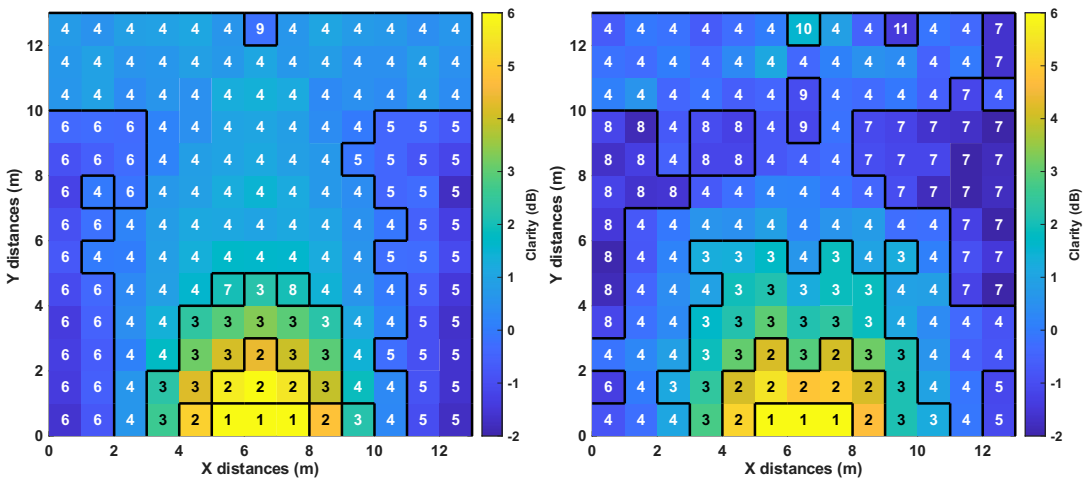

(a) Simulation **(b)** Measurement

Figure 5: Heatmap of C_{80} ISO single number values, averaged over 500 Hz and 1000 Hz octave bands for simulated and measured positions. Color represents parameter values and numbers identify the JND-informed regions using a 2 JND threshold.

the source. The simulated data is divided into bands extending across the width of the room. The measured data present more local variation with less regular region limits. The measured grid was divided into 18 JND-informed regions, compared to 7 regions in the simulation. Therefore, the distribution of the simulated J_{LF} has substantially fewer and larger perceptual regions.

4. Discussion

The results of both methods indicate that the simplified room acoustic simulation captures the overall spatial organization of the measured data, while local variations were generally underrepresented. In Method A, the simulated and measured data showed comparable spatial changes in the estimated perceived source direction, especially in the lateral and front-lateral receiver positions. The simulation produced fewer directional regions than the measurement, especially when estimated sound intensity was included. A similar trend was observed in Method B: the main spatial organization of C_{80} and J_{LF} was reproduced, but the simulation presented a smoother spatial variability, with fewer and larger JND-informed regions. The parallel between the two methods suggests that a simplified simulation can provide relevant estimates of broad spatial characteristics, although it may not reproduce the detailed variability of the measured dataset.

For Method A, extending the analyzed RIR portion from the direct sound to the first 5 ms resulted in only small changes in the number of predicted regions. For this experimental setup, this interval includes primarily the floor reflection, and as expected, it had little effect on the estimated perceived direction. This method therefore provides a relatively stable and intuitive subdivision of the receiver grid and if considered in isolation it would suggest that the measurement positions could be determined primarily from source-receiver localization related cues. However, the accuracy of Method A depends primarily on the auditory model used to estimate perceived DOAs, which is still an ongoing research area. Method B shows that this interpretation is incomplete when the complete room response is considered. The resulting regions depend strongly on the selected room acoustic parameter. While the measured and simulated C_{80} receivers were divided into 11 and 9 regions, J_{LF} needed 18 and 7 regions. The spatial arrangement of the regions also differed considerably, with C_{80} suggesting more regions closer to the source and J_{LF} dividing the grid into a large and smooth frontal area. Therefore, a grid that may appear solved when perceived-direction is considered may not properly represent other perceptual attributes.

The smoother simulated distribution may result from the simplified geometry, material choice, source directivity, and the statistical treatment of scattering in the GA modeling. Diffraction and other wave-related effects are also approximated or omitted, which may contribute to the reduced local variability. The simulations should perhaps not be used blindly for defining the spatial sampling of a room, which may also depend on the intended application (e.g., immersive experiences [23]). Nevertheless, the agreement in the broader spatial tendencies supports the use of simulations to inform decisions during a measurement campaign. A practical measurement strategy may therefore combine the different approaches and choose the finest spatial sampling of different room acoustic parameters.

5. Summary and Conclusion

Both methods indicate that a simplified GA simulation can reproduce the broad spatial variation of the measured sound field, although it tends to underestimate local spatial variability. The perceived-direction method offers a promising basis for identifying appropriate measurement regions, while the JND-informed analysis shows that the required spatial resolution depends strongly on the room acoustic parameter under consideration. Overall, our findings suggest that simplified room simulations have the potential to reduce measurement effort by providing an informed, pre-measurement estimate of the spatial sampling required.

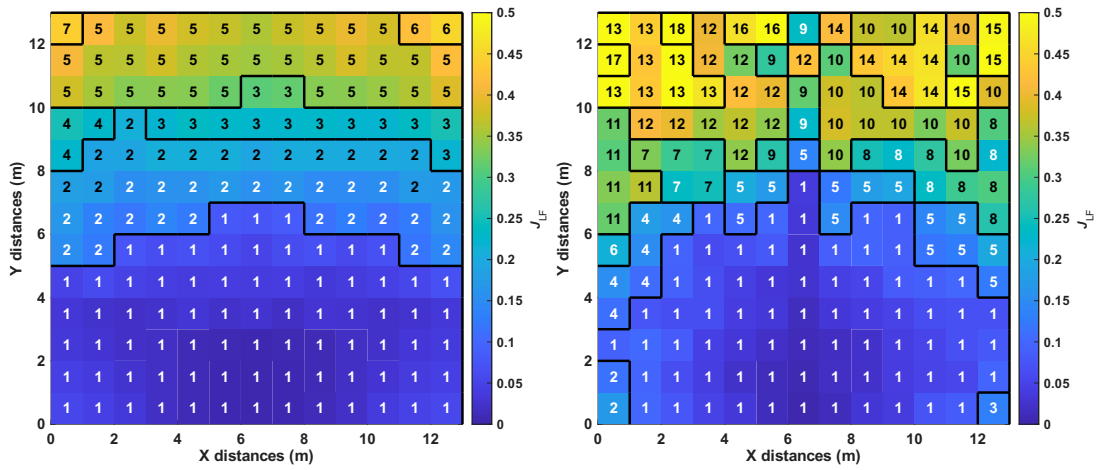

(a) Simulation **(b)** Measurement

Figure 6: Heatmap of J_{LF} ISO single number values, averaged over the 125-1000 Hz octave bands, for simulated and measured receiver positions. Color represent parameter values and numbers identify JND-informed regions using a 2 JND threshold.

References

[1] I. B. Witew, M. Vorländer, and N. Xiang. "Sampling the sound field in auditoria using large natural-scale array measurements". In: *JASA* 141.3 (2017).

[2] G. Götz et al. "Autonomous Robot Twin System for Room Acoustic Measurements". In: *JAES* 69 (2021).

[3] G. Stolz et al. "Autonomous robotic platform to measure spatial room impulse responses". In: *Proc. DAGA*. Hamburg, Germany, 2023.

[4] ISO. *ISO 3382 Measurement of room acoustic parameters*. Geneva, CH, 2009.

[5] G. Stolz et al. "Discussion of acoustic and perceptual optimization methods for measuring spatial room impulse responses with a mobile robotic platform". In: *I3DA*. Bologna, Italy, 2023.

[6] J. Blauert. *Spatial hearing: the psychophysics of human sound localization*. MIT press, 1997.

[7] R. Y. Litovsky et al. "The precedence effect". In: *JASA* 106.4 (1999).

[8] W. M. Hartmann. "Localization of sound in rooms". In: *JASA* 74.5 (1983), pp. 1380–1391.

[9] L. L. Beranek. *Music, acoustics & architecture*. John Wiley & Sons, 1962.

[10] R. Adams and L. Bischof. "Seeded Region Growing". In: *IEEE Trans. Pattern Anal. Mach. Intell.* 16.6 (1994).

[11] R. Stewart and M. Sandler. "Database of omnidirectional and B-format room impulse responses". In: *ICASSP*. Dallas, US, 2010.

[12] M. Vorländer. *Auralization: Fundamentals of Acoustics, Modelling, Simulation, Algorithms and Acoustic Virtual Reality*. Springer, 2008.

[13] A. James. *The Norwich Forum—The Acoustics of a Library for the 21st Century*. Adrian James Acoustics. 2001.

[14] A. Pilch. "Optimization-based method for the calibration of geometrical acoustic models". In: *Applied Acoustics* 170 (2020). ISSN: 1872910X.

[15] D. Lee, D. Cabrera, and W. L. Martens. "The effect of loudness on the reverberance of music: Reverberance prediction using loudness models". In: *JASA* 131.2 (2012).

[16] C. L. Christensen and J. H. Rindel. "A new scattering method that combines roughness and diffraction effects Geometrical model The Reflection Based Scattering coefficient". In: *Forum Acusticum*. Budapest, Hungary, 2005.

[17] D. Schröder and M. Vorländer. "RAVEN: A real-time framework for the Auralization of interactive virtual environments". In: *Forum Acusticum*. Aalborg, Denmark, 2011.

[18] A. Gallien, K. A. Prawda, and S. J. Schlecht. *Sound-source directivity dataset for four loudspeakers*. Zenodo, 2023.

[19] M. Dietz, S. D. Ewert, and V. Hohmann. "Auditory model based direction estimation of concurrent speakers from binaural signals". In: *Speech Communication* 53.5 (2011), pp. 592–605.

[20] P. Majdak, C. Hollomey, and R. Baumgartner. "AMT 1.x: A toolbox for reproducible research in auditory modeling". In: *Acta Acust.* 6 (2022).

[21] C. Armstrong et al. "A Perceptual Evaluation of Individual and Non-Individual HRTFs: A Case Study of the SADIE II Database". In: *Applied Sciences* 8.11 (2018).

[22] S. Tervo. *SDM Toolbox*. `https://mathworks.com/matlabcentral/fileexchange/56663-sdm-toolbox`. 2016.

[23] N. Zheng, N. Peters, and E. Bates. "On the relationship between objective room acoustic parameters and perceived differences in spatially interpolated RIRs". In: *I3DA*. Bologna, Italy, 2025.